# IMPACT OF EDGE ELECTRIC FIELDS ON PARTICLE TRANSPORT AND DYNAMICS IN TOKAMAKS

O. DUMBRAJS, J.A. HEIKKINEN, S.J. KARTTUNEN, T.P. KIVINIEMI, T. KURKI-SUONIO, T.J.H. PÄTTIKANGAS, K.M. RANTAMÄKI, S. SAARELMA, R.R.E. SALOMAA, S. SIPILÄ, T.J.J. TALA, P. BIBET[1], X. LITAUDON[1], D. MOREAU[1], A. PEETERS[2], A. EKEDAHL[3]

Association Euratom-Tekes, Helsinki University of Technology and VTT Energy, Finland
[1]Association Euratom-CEA, Cadarache, France
[2]Association Euratom-IPP, Garching, Germany
[3]JET Joint Undertaking, Abingdon, Oxfordshire, OX14 3EA, UK

**Abstract**

Three aspects of tokamak edge physics are addressed. Role of radial electric field and poloidal rotation at the L-H transition is investigated with the Monte Carlo code ASCOT. Ripple ions and their use in measuring edge electric field are studied. Generation of fast electrons and hot spots in the lower hybrid grill region by the RF electric field is investigated with particle-in-cell simulations.

## 1. ORBIT LOSS MODEL IN L-H TRANSITIONS

For tokamak plasmas, the neoclassical transport theory gives the minimum particle and heat flux in a real experiment but, in most conditions, the anomalous transport is the dominant mechanism. The dependence of the neoclassical flux on a radial electric field $E_r$ can be modelled analytically, but while the anomalous flux still lacks an analytical expression, it has been observed to be suppressed in the presence of $E_r$. An interesting link between the two fluxes is provided by the theory [1] which proposes that the jump in the radial electric field during an L-H transition could be due to a multivalued balance between ion orbit loss current and the neoclassical return current at the edge of a tokamak. The 5D Monte Carlo code ASCOT [2] offers an ideal tool to simulate both of these currents. ASCOT is used to verify the existing expressions for the neoclassical return current, and to simulate the ion orbit loss current in a real tokamak geometry.

In Fig. 1(a), the neoclassical current from two different expressions [1, 3] is compared to the simulations. The simulated current is obtained by initialising the test particles according to the background density profile and calculating the crossings of the test particles over the flux surfaces. In the simulations, test particles scatter from the background, and the momentum non-conserving collision operator ensures that the parallel velocity remains small. (The same is assumed in deriving the analytical formulas). The simulation is done in circular geometry in plateau regime with temperature $T = 150$ eV, and density $n = 5 \times 10^{19}$ m$^{-3}$, corresponding to normalized collisionality $\nu_{\mathrm{i}}^* = 23$. Toroidal magnetic field is $B_{\mathrm{t}} = -2.5$ T, and the plasma current is $I_{\mathrm{p}} = 1$ MA. Qualitatively the results do agree, but there are quantitative differences due to the simpler collision operator and various other approximations used in deriving the analytical expressions.

In Fig. 1(b), the maximum value of the neoclassical current from the analytical expression [1] is compared with the simulated ion orbit loss current for $E_r = 0$. The comparison is given as a function of the normalized collisionality. A bifurcation is assumed to happen at the crossing point of the curves. In the simulation, H-mode data of the ASDEX Upgrade discharge #8044 is used, and the different collisionalities are obtained by multiplying the temperature profile by a constant factor. In a good agreement with the analytic theory, figure shows the balance between the two currents when $\nu_{\mathrm{i}}^*$ is near unity and for real experimental conditions the ion orbit loss is far too small to explain the transition.

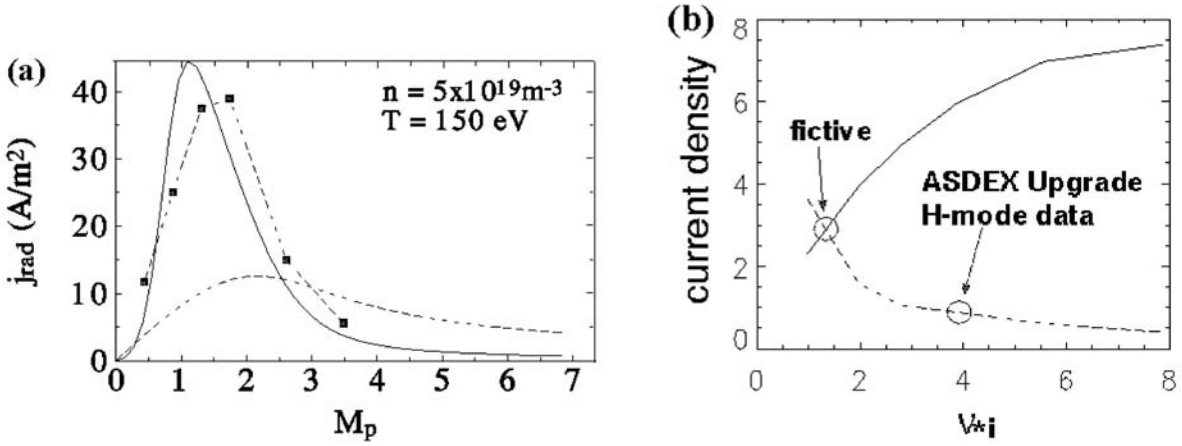


*FIG. 1: (a) Comparison of numerically calculated neoclassical current (dashed line with boxes) to the analytical ones from Ref. [1] (dashed line without boxes) and Ref. [3] (solid line) as a function of radial electric field. (b) Orbit loss current and the neoclassical return current as a function of collisionality.*

## 2. CX DIAGNOSTICS OF RADIAL ELECTRIC FIELD AT L-H TRANSITIONS

A radial electric field is believed to play a crucial role in triggering the L-H transition. The time resolution of the spectroscopic measurements, currently used for probing the dynamics of the L-H transition, has not yet been good enough (about 0.5 ms) to decide whether the changes in $E_r$ are sufficiently fast, and if they indeed precede the L-H transition. Experiments at ASDEX Upgrade [4] have found that the neutral fluxes from ripple-trapped slowing-down beam ions grow by a factor 10–30 at an L-H transition. The growth was also observed to depend on the energy of the detection channel. Therefore, if the growth in the neutral fluxes resulting from charge exchange (CX-) reactions were due to changes in $E_r$, the CX-signal might provide a faster diagnostic (time resolution $< 100\mu$s) for the radial electric field.

ASCOT simulations of ripple-trapped beam ions [5, 6] verify that the CX-signal strongly responds to a radial electric field: the CX-flux characteristics are reproduced for experimental conditions. Figure 2 shows the simulated CX-signal enhancement due to $E_r$, $\Gamma(E_r \neq 0)/\Gamma(E_r = 0)$, as a function of the toroidal and poloidal angles. The enhancement is shown for two different widths of the $E_r$-profile. The initial energy of the test particles (deuterons) is 20 keV, which is one-third of the beam's nominal energy. The pitch ($\xi = v_\parallel/v$) of the ions contributing to the signal in Fig. 2, satisfies the condition $|\xi| < 0.07$, and their kinetic energy lies between 5 and 15 keV. With $E_r = 0$, the signal is found to have a significant deficit near the bottom of the magnetic well, where the detected ions are trapped. Poloidally, the signal is much stronger in the lower half, in agreement with the downward drift of the ripple ions. When $E_r$ is introduced, the depression around the bottom of the magnetic well not only disappears, but the signal now has its maximum there. The enhancement increases with the widening of the $E_r$-profile. The response time to the onset of the radial electric field is typically less than 50 (s. The filling of the depleted region can be explained by the different ripple-ion drift orbit topologies generated by $E_r$, and the time scale is determined by the convective drift time from the inner, well-filled ripple region to the depleted region along these orbits [7]. Consequently, the time scale can be much faster than the collisional time scale, and the ripple-ion population should faithfully follow the changes in $E_r$.

According to Fig. 2, the presence of $E_r$ can be best observed by monitoring the ripple-blocked ions near the bottom of the ripple well, for a relatively narrow poloidal range around the midplane. Ripple-ions with energies below a certain maximum, set by the strength of $E_r$, will respond to the electric field. In the ASDEX Upgrade experiments [4] the CX-signal was found to

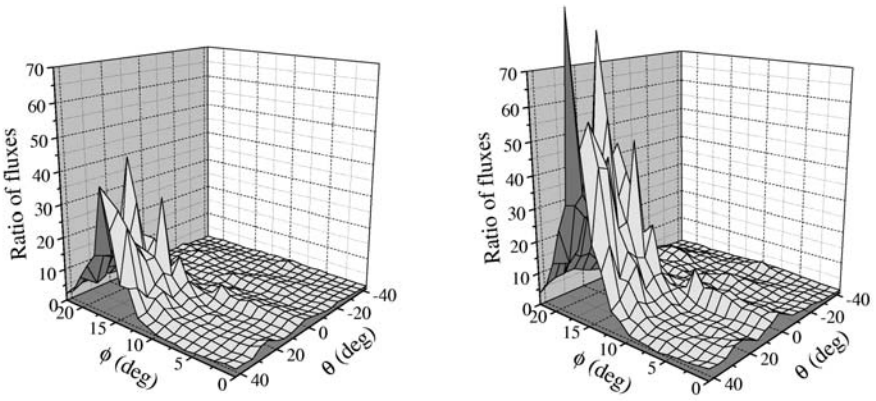


*FIG. 2: Simulated CX-signal enhancement (ASDEX Upgrade shot 8044 at $t = 1.3$ s) due to $E_r$ given by a Gaussian potential, $V = V_0 e^{-(r-a)/w}$, with $V_0 = 200$ V. In (a) $w = 1$ cm, and in (b) $w = 2$ cm.*

start growing the later the larger the energy of the detection channel was, indicating a steadily growing electric field after the L-H transition. At first sight, the slow (1 ms) evolution of the CX-signal observed in Ref. [4] does not appear consistent with a fast jump in the radial electric field. However, because according to the simulations, the CX-signal enhancement becomes stronger for wider and stronger fields (up to some saturation width and strength), a modest fast jump of the field could remain undetected. Comparison of our simulations with the experimental findings [4] supports a picture in which $E_r$ can experience a modest fast jump just within 1 cm of the separatrix, followed by a later, much slower ($> 1$ ms) growth and broadening of the profile.

## 3. GENERATION OF FAST ELECTRONS AND HOT SPOTS IN THE LH GRILL REGION

In lower hybrid (LH) current drive experiments at Tore Supra and Tokamak de Varennes (TdeV), hot spots and generation of impurities have been observed on components magnetically connected to the grill region [8]. A possible explanation is the parasitic absorption of LH power near the grill mouth resulting in a population of fast electrons [9].

We investigate the parasitic absorption of LH power in the near field of the LH grills of ITER, JET and Tore Supra with the 2d3v electrostatic particle-in-cell (PIC) code XPDP2 [10, 12]. The code is periodic in the toroidal direction and bounded in the radial direction. The static magnetic field is assumed to lie along the toroidal axis together with the grill mouth. In order to model experiments with realistic wave spectra, XPDP2 was coupled with the SWAN code [11] through a surface charge [13]. In front of the grill, a linear density profile was assumed. The simulation parameters are summarised in Table I.

Figure 3 shows the absorption profiles for the three devices. The absorption occurs within a few millimetres in front of the launcher. The simulations show that the parasitic absorption is fairly weak in ITER and fairly strong in Tore Supra at high intensities.

In the PIC simulations, the coupled power densities were 25–82 MW/m$^2$. For ITER the absorbed power density in the near field of the launcher was found to be only 14 kW/m$^2$ even though the coupled power density was 82 MW/m$^2$, which is much larger than the design value of 23 MW/m$^2$. The reason for this is that the spectrum of the ITER launcher has only small amount of power at high-$n_\parallel$. In the simulations for JET, the absorbed power was also rather small, 65–210 kW/m$^2$. This is mainly because the coupled power densities that were considered were rather low, 25–30 MW/m$^2$. In the simulations for Tore Supra, the coupled power densities were 35–50 MW/m$^2$. The parasitic absorption in front of the launcher was 270–420 MW/m$^2$.

TABLE I: SIMULATION PARAMETERS FOR ITER, JET AND TORE SUPRA ($T_e = 25$ eV).

| | ITER | JET | | Tore Supra | | | |
|---|---|---|---|---|---|---|---|
| Edge density, $n_{e0}$ [$10^{18}$ m$^{-3}$] | 1.0 | 0.3 | 3.0 | 0.6 | 1.0 | 1.5 | 2.0 |
| Density scale length, $n_{e0}/n'_e$ [cm] | 1.0 | 1.0 | 1.0 | 0.6 | 1.0 | 1.5 | 2.0 |
| Magnetic field, $B$ [T] | 4.0 | 2.2 | | | 2.78 | | |
| Grill frequency, $\nu$ [GHz] | 5.0 | 3.7 | | | 3.7 | | |
| Coupled intensity, $I_{in}$ [MW/m$^2$] | 82 | 30 | 25 | 48 | 50 | 35 | 36 |
| Parasitic absorption, $I_{abs}$ [kW/m$^2$] | 14 | 65 | 210 | 350 | 420 | 280 | 270 |
| Electron energies, $E_{e,kin}$ [keV] | 0.3 | 0.4 | 0.4 | 1.6 | 1.4 | 0.6 | 0.5 |

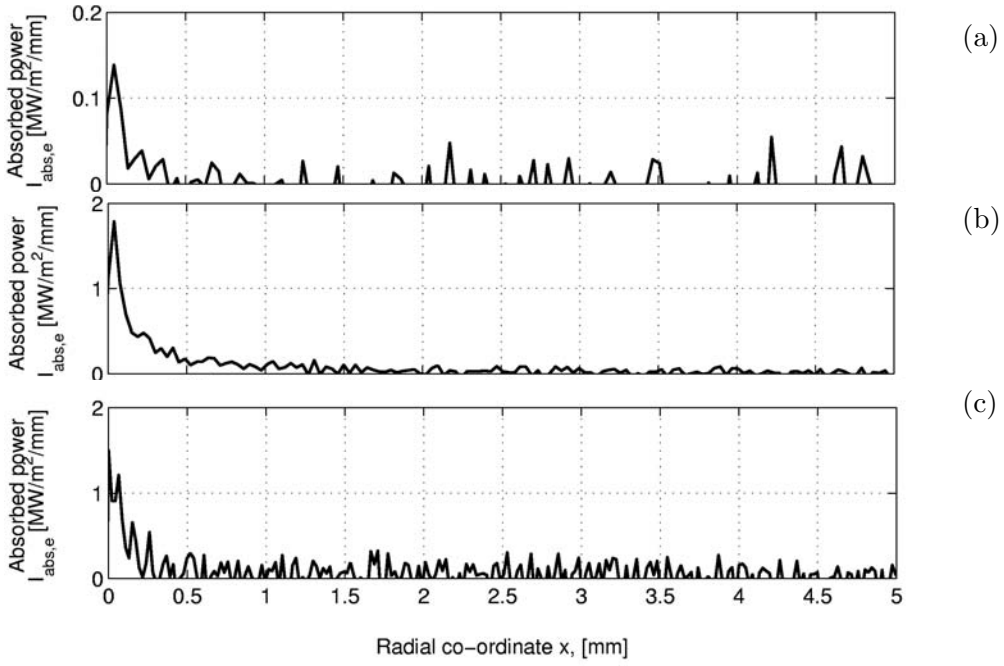


*FIG. 3: Absorbed power density per unit length versus radial co-ordinate in (a) ITER, (b) Tore Supra ($n_{e0} = 1 \times 10^{18}$ $m^{-3}$) and (c) JET ($n_{e0} = 3 \times 10^{18}$ $m^{-3}$).*

A significant amount of fast electrons was generated for Tore Supra when the coupled power density was large ($> 45$ MW/m$^2$). The maximum energies were about 1.6 keV. The results are summarised in Table I.

One should note that the lower hybrid launchers of JET and Tore Supra are very similar. In the simulations, a higher amount of parasitic absorption was found for Tore Supra mainly because the LH intensities used in the simulations were higher for Tore Supra than for JET.

## REFERENCES


[1] SHAING, K.C., et al., Phys. Rev. Lett. **63** (1989) 2369.
[2] HEIKKINEN, J.A., SIPILÄ, S.K., Phys. Plasmas **2** (1995) 3724.
[3] STRINGER, T.E, CONNOR, J.W., Phys. Fluids **14** (1971) 2177.
[4] HERRMAN, W., Phys. Rev. Lett. **75** (1995) 4401.
[5] HEIKKINEN, J.A., HERRMAN, W., KURKI-SUONIO, T., Phys. Plasmas **4** (1997) 3655.
[6] HEIKKINEN, J.A., HERRMAN, W., KURKI-SUONIO, T., Nucl. Fusion **3** (1998) 419.
[7] HEIKKINEN, J.A., KURKI-SUONIO, T., Phys. Plasmas **5** (1998) 692.
[8] MAILLOUX, J., DEMERS, Y., FUCHS, V., et al., J. Nucl. Mater. **241–243** (1997) 745.
[9] FUCHS, V., GONICHE, M., DEMERS, Y., et al., Phys. Plasmas **3** (1996) 4023.
[10] VAHEDI, V., BIRDSALL, C.K., LIEBERMAN, M.A., et al., Phys. Fluids **B 5** (1993) 2719.
[11] MOREAU, D., et al., Radiation in Plasmas, Vol. 1 (MCNAMARA, B., Ed.), World Scientific (1984), p. 331.
[12] RANTAMÄKI, K.M., PÄTTIKANGAS, T.J.H., et al., Phys. Plasmas **5** (1998) 2553.
[13] RANTAMÄKI, K.M., PÄTTIKANGAS, T.J.H., et al., Europhys. Conf. Abstr. **22A** (1998) 173.